Two structurally distinct domains of the nucleoporin Nup170 cooperate to tether a subset of nucleoporins to nuclear pores

Dirk Flemming,[1] Phillip Sarges,[1] Philipp Stelter,[1] Andrea Hellwig,[2] Bettina Böttcher,[3] and Ed Hurt[1]

[1]Centre for Biochemistry and [2]Department of Neurobiology, University of Heidelberg, D-69120 Heidelberg, Germany
[3]The School of Biological Sciences, University of Edinburgh, Edinburgh EH9 3JR, Scotland, UK

How individual nucleoporins (Nups) perform their role in nuclear pore structure and function is largely unknown. In this study, we examined the structure of purified Nup170 to obtain clues about its function. We show that Nup170 adopts a crescent moon shape with two structurally distinct and separable domains, a β-propeller N terminus and an α-solenoid C terminus. To address the individual roles of each domain, we expressed these domains separately in yeast. Notably, overexpression of the Nup170 C domain was toxic in *nup170Δ* cells and caused accumulation of several Nups in cytoplasmic foci. Further experiments indicated that the C-terminal domain anchors Nup170 to nuclear pores, whereas the N-terminal domain functions to recruit or retain a subset of Nups, including Nup159, Nup188, and Pom34, at nuclear pores. We conclude that Nup170 performs its role as a structural adapter between cytoplasmically oriented Nups and the nuclear pore membrane.

Introduction

The nuclear pore complex (NPC) is a supramolecular assembly that is inserted in the nuclear envelope (NE) and mediates nucleocytoplasmic transport (Fahrenkrog and Aebi, 2003; Tran and Wente, 2006). The NPC scaffold is characterized by distinct substructures that are arranged with an eightfold rotational symmetry (Stoffler et al., 1999; Beck et al., 2007). The NPC in the yeast *Saccharomyces cerevisiae* is ∼60 MD in size and consists of multiple copies of ∼30 different proteins called nucleoporins (Nups; Rout et al., 2000).

One of the major structural components of the NPC is Nup170, which is required for the maintenance of a normal NPC structure and is implicated to have a role in NPC biogenesis (Aitchison et al., 1995). Nup170 and its highly related homologue Nup157 were identified in a synthetic lethal screen using the nuclear pore membrane protein Pom152. Neither *NUP157* nor *NUP170* are essential, but deletion of both genes caused a lethal phenotype. Genetic analyses showed that a *nup170Δ pom152Δ* double mutant was lethal, whereas the combination *nup157Δ pom152Δ* allowed cell growth. Repression of *NUP170* in a *pom152Δ* background induced the formation of an irregularly shaped NE with massive extensions and invaginations. In addition, structures interpreted as partially assembled NPCs were described in the respective strains to be located below the double membrane (Aitchison et al., 1995). Nup170 was shown to be required for normal stoichiometry of FG Nups and to be involved in localizing specific FG Nups (e.g., Nup1 and Nup2) within the NPC (Kenna et al., 1996). Moreover, Nup170 forms a complex with Nup53 and Nup59 and also associates with the nuclear transport receptor Kap121 (Marelli et al., 1998). Nup53 itself was shown to interact with Ndc1, which is another nuclear pore membrane protein, suggesting that Nup53 could bridge between the NPC core and the pore membrane, making it a prime candidate to affect both nuclear pore membrane and NPC biogenesis in conjunction with Nup170 (Galy et al., 2003; Mansfeld et al., 2006; Hawryluk-Gara et al., 2008). Consistent with this possibility, overproduction of Nup53 disturbed NE organization (Marelli et al., 2001). Nup170, as well as Nup188, another large structural Nup, has also been implicated in the control of NPC permeability by altering the diameter for passive diffusion in *nup170Δ* cells (Shulga et al., 2000).

D. Flemming and P. Sarges contributed equally to this paper.

Correspondence to Ed Hurt: ed.hurt@bzh.uni-heidelberg.de

Abbreviations used in this paper: FAS, fatty acid synthase; NE, nuclear envelope; NPC, nuclear pore complex; Nup, nucleoporin; TEV, tobacco etch virus; SDC, synthetic dextrose complete; SRC, synthetic raffinose complete.

The Rockefeller University Press $30.00
J. Cell Biol. Vol. 185 No. 3 387–395
www.jcb.org/cgi/doi/10.1083/jcb.200810016

Nup157 and Nup170, both belonging to the large structural Nups, are predicted to contain an N-terminal β-propeller and a C-terminal α-solenoid domain (Devos et al., 2006). Although both proteins are highly similar and have overlapping functions, they also have unique roles. For example, Nup170 is involved in chromosome segregation and kinetochore function, which was not found for Nup157 (Kerscher et al., 2001). Recently, Nup170 was suggested to be located adjacent to the center of the nuclear membrane curvature and thus could play a role in the buildup of the NPC scaffold (Alber et al., 2007).

Knowledge of a detailed structural buildup of Nups at the atomic level is still limited, although x-ray structures of scaffold NPC components are emerging (Hodel et al., 2002; Berke et al., 2004; Weirich et al., 2004; Melcak et al., 2007). The largest structure so far of a single Nup (Nic96) was solved recently and showed deviations from the predicted α-solenoid fold (Jeudy and Schwartz, 2007; Schrader et al., 2008). Structural analysis of full-length Nups was only performed by EM, and a first 3D reconstruction of Nup157 revealed a crescent-shape structure (Lutzmann et al., 2005).

In this study, we determined the structure of full-length Nup170 by EM. Nup170 has a crescent-shaped morphology with two structurally distinct and separable domains. The overproduction of the C-terminal domain of Nup170 induces a toxic phenotype in *nup170Δ* cells. Concomitant to Nup170C overexpression, several other Nups, including Nup159, Nup82, Nup188, and Pom34, were mislocalized to cytoplasmic foci. This toxicity of Nup170C was reversed by coexpression of Nup170N, which led to an interaction between both domains and assembly into intact NPCs. Our data provide insight into the anatomy of a large structural Nup with respect to domain organization, NPC targeting and maintenance, and stability of the NPC.

Results and discussion

Nup170 has a crescent-shaped structure

To gain insight into the Nup170 morphology with respect to the arrangement of the structurally predicted N and C domains, we sought to determine its 3D structure by EM. Expression and purification of Nup170 from *Escherichia coli* was not possible because the recombinant protein had the tendency to aggregate. However, a functional Nup170 protein genomically tagged with protein A–tobacco etch virus (TEV)–Flag could efficiently be purified from yeast with only a minor contamination of fatty acid synthase (FAS; Fig. 1 A, left). This purified Nup170 was subjected to EM analysis by performing negative staining with uranyl acetate and imaging under low dose conditions.

The micrographs showed monodisperse particle distributions slightly contaminated by FAS (see previous paragraph). Because of its characteristic morphology, the FAS did not interfere with the subsequent image processing. The particle images revealed different views of Nup170 without a preferential orientation, ranging from a globular to a crescent-like morphology (Fig. 1 A, right). For the calculation of a 3D map, a series of micrographs were recorded, and particle images were selected from the micrographs and aligned to sets of multiple references. Alignment to selected classes followed by classification was repeated until stable classes were obtained (Fig. 1 B, top row). We assumed that these class averages corresponded to different projections of a unique 3D shape, and, consequently, the class averages were combined to a 3D map by back projection (Fig. 1 B, middle and bottom rows). The accuracy of the map was tested by comparison of the class averages and the related reprojections of the 3D map. For the displayed volume, the class averages agreed reasonably well with the corresponding reprojections.

The calculated 3D structure revealed that Nup170 has a crescent-shaped morphology with one end of the crescent being significantly thicker than the other (Fig. 1, B and C; and Video 1). The overall dimensions of the particle were 13 nm in length and 8 nm in width. The morphology of Nup170 determined in this study resembles that of Nup157 with a similar crescent shape (Lutzmann et al., 2005). Superposition of the volumes of Nup170 and Nup157 showed the same curvature between the thicker end and the rest of the particle for both Nups, with the thinner end being somewhat longer in Nup170. Considering the general problems of reconstructing structures of low molecular weight complexes, the differences in the details of the maps of Nup157 and Nup170 most likely reflect inaccuracies in the image reconstructions rather than genuine differences in the architecture of the both molecules, which are highly homologous.

Next, we determined the EM structure of the C-terminal domain of Nup170. In this case, protein A–tagged Nup170C (residues 755–1,502) was expressed in *E. coli* and purified to homogeneity (Fig. 1 D). Nup170C was significantly shorter than full-length Nup170 but still exhibited the characteristic bending (Fig. 1 D). However, the prominent mass present on the thick arm of the full-length Nup170 crescent was absent in Nup170C, suggesting that this part corresponds to the Nup170 N domain (Fig. 1 C). Consistent with this interpretation, the predicted N-terminal β-propeller and the C-terminal α-solenoid domain of Nup170 (Devos et al., 2006) could be manually fitted, respectively, into the bulbous end and the rest of the bend structure of the full-length Nup170 EM volume (Fig. 1 C). Altogether, the structural data suggest that the C domain of Nup170 can fold independently from the N domain and thus could perform separate functions.

Overexpression of the Nup170 C domain is toxic but can be rescued by coexpression of either Nup170N or Nup157N

To find out whether distinct functions can be assigned to the Nup170 N and C domains, we expressed the separate domains in yeast. *NUP170* is not essential in yeast, and *nup170Δ* cells have a mildly impaired cell growth (Fig. 2 A; Aitchison et al., 1995). To find out whether an overproduction of Nup170 interferes with normal NPC biogenesis, we overexpressed full-length *GAL::NUP170* in *nup170Δ* cells grown but did not observe an impaired cell growth (Fig. 1 A; Aitchison et al., 1995). However, when the Nup170 C-terminal domain (i.e., the predicted α-solenoid; aa 721–1,502) was overexpressed in *nup170Δ* cells, cell growth was inhibited (*GAL::NUP170C*; Fig. 2 A). In contrast, overproduced *GAL::NUP170C* was not toxic in *NUP170* wild-type cells (Fig. S1). Moreover, an overproduced *GAL::NUP170N* construct (i.e., the predicted β-propeller; aa 1–720)

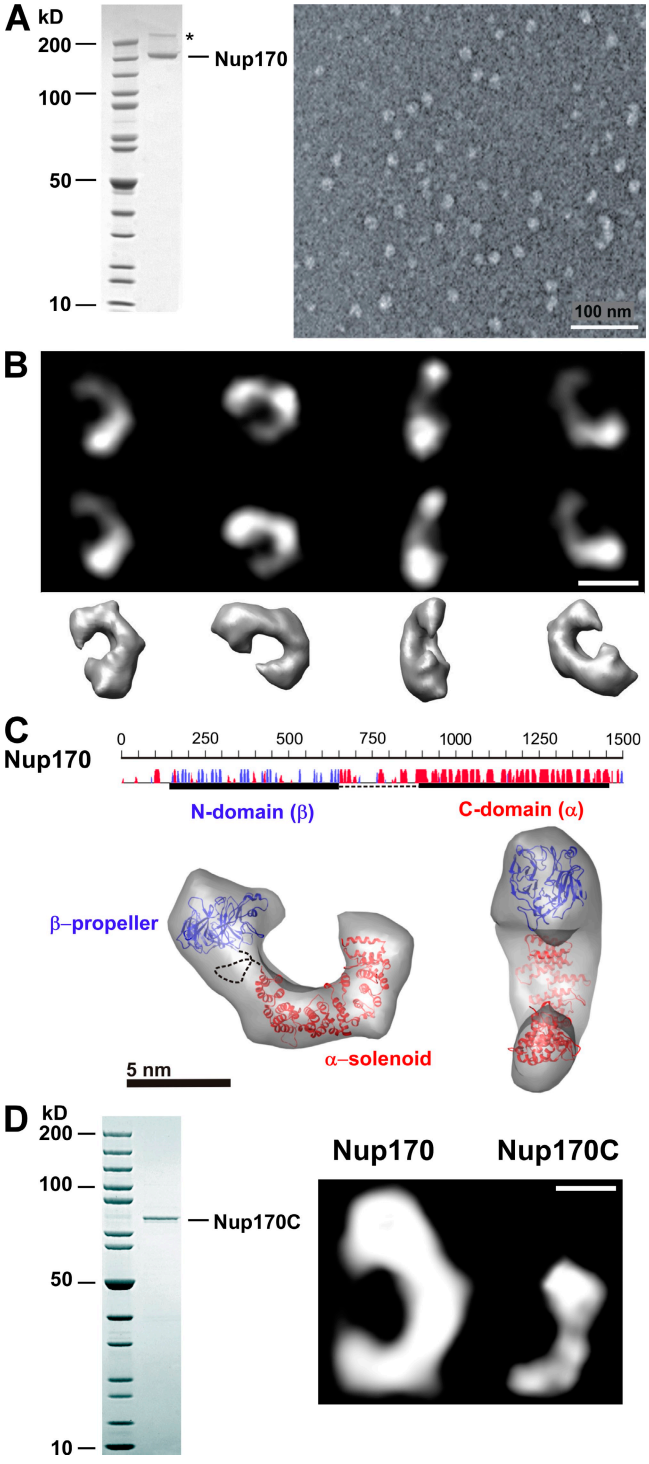

Figure 1. **Electron microscopic single-particle analysis of purified full-length Nup170 and Nup170C.** (A) Affinity-purified Nup170 was analyzed by SDS-PAGE and Coomassie staining (left; contaminated by FAS and indicated by an asterisk) and by EM (right). A charge-coupled device image overview electron micrograph of the negatively stained Nup170 is shown. (B) Class averages (top), corresponding reprojections of the final 3D model (middle), and surface representations of Nup170 in equivalent orientations (bottom) are shown. (C) Modeling the Nup170 sequence with its predicted β-strands (purple; residues 144 to 648) and α-helices (red; residues 890 to 1,460; loops bigger than 12 aa were omitted) according to Devos et al. (2006) into the 3D EM structure of the Nup170. The β-propeller and α-solenoid were manually fitted into the 3D shape of the crescent-shaped Nup170 molecule. The dashed line indicates a putative unstructured region between the β-propeller and α-solenoid domains, ~240 aa in length, for which a secondary structural prediction was not obtained. (D) SDS-PAGE of the purified C-terminal domain of Nup170 (left) and comparison of representative class averages of Nup170C with a projection of Nup170 full-length at the same scale (right). Bars: (B) 4.5 nm (D) 2.9 nm.

did not impair growth of *nup170Δ* cells but could rescue in trans the lethal phenotype of *GAL::NUP170C* (Fig. 2 A). These data indicate that overexpression of the Nup170 C domain specifically induces a toxic phenotype in cells lacking *NUP170*.

Unexpectedly, Nup157C overexpressed from the *GAL* promoter did not cause a significant toxic phenotype, neither in *nup170Δ* nor in *nup157Δ* cells (Fig. 2, B and C). However, induction of *GAL::NUP157N* could rescue the toxic phenotype of Nup170C overexpression (Fig. 2 B). This finding suggests that the N domains of Nup170 and Nup157 can replace each other to neutralize the toxicity of the overproduced Nup170 C domain.

To find out how overproduced Nup170C could induce a toxic phenotype in *nup170Δ* cells, we investigated the NE targeting of GFP-labeled Nup170 constructs. In this case we expressed Nup170C under the control of the constitutive *NOP1* promoter, which is less strong than the *GAL* promoter. Accordingly, *NOP1::NUP170C* was less toxic and exhibited a reduced expression when compared with *GAL::NUP170C* (Fig. 2 D and Fig. S1). In *NUP170* wild-type cells, GFP-Nup170C expressed from the *NOP1* promoter significantly accumulated in the nucleus with no sign of an NE association (Fig. 3 A), whereas in *nup170Δ* cells, GFP-Nup170C exhibited a punctate NE staining (Fig. 3 A). Besides this predominant NPC location, Nup170C-GFP was occasionally seen in a cytoplasmic spot (Fig. 3 A; see next section). In contrast, Nup170N was evenly distributed between the nucleus and cytoplasm in *nup170Δ* cells, but was efficiently targeted to the NE upon coexpression of Nup170C (Fig. 3 A). These findings indicate that Nup170C did not assemble into NPCs in the presence of chromosomal *NUP170*, suggesting that endogenous Nup170 competes with Nup170C for a binding site in the NPC. Nup170C is incorporated into NPCs in the absence of endogenous Nup170, pointing to the importance of the α-solenoid in anchoring Nup170 to the NPC.

The observations that Nup170N can rescue the toxic phenotype of Nup170C in trans and that the separated Nup170N is targeted to the NE upon Nup170C coexpression suggested that both domains can physically interact. Consistent with this possibility, the N and C domains of Nup170 interact with each other in vivo as shown by two-hybrid analysis (Fig. 3 B) and coprecipitation using protein A–tagged Nup170C and myc-tagged Nup170N (Fig. 3 C).

Nup170C overproduction induces accumulation of a subset of Nups in cytoplasmic foci

To find out whether the toxic overexpression of Nup170C affects assembly and/or structure of the NPC, we analyzed the location of chromosomally integrated GFP-tagged Nups in *nup170Δ* cells. Most of the GFP-tagged Nups exhibited a normal punctate NE staining in *nup170Δ* cells when *GAL::NUP170C* was not induced. Only Nup82-GFP (Fig. 4) and

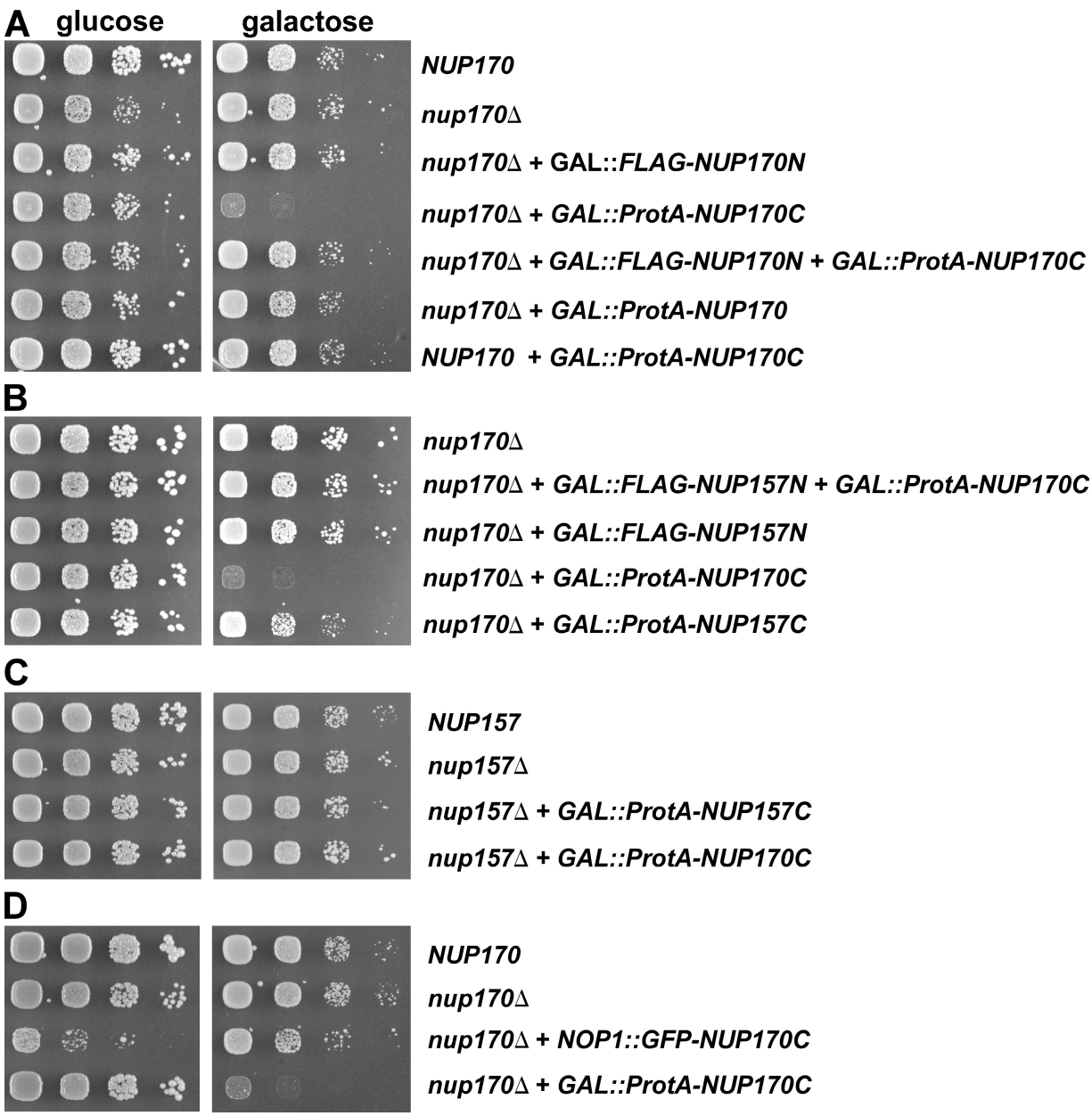

Figure 2. **Overexpression of *GAL::NUP170C* causes a toxic phenotype in *nup170Δ* cells.** (A) Full-length Nup170 and the indicated tagged Nup170C and Nup170N domains were overexpressed in either wild-type (*NUP170*) or *nup170Δ* cells. (B) The indicated Nup157N, Nup157C, and Nup170C domains were overexpressed under the control of the *GAL* promoter in *nup170Δ* cells. (C) The indicated Nup157C or Nup170C domains were overexpressed under the control of the *GAL* promoter in *nup157Δ* cells. (D) Nup170C was expressed either under the control of the *GAL* promoter or the *NOP1* promoter in *nup170Δ* cells. Cells were spotted in 10-fold serial dilutions on glucose-containing plates (noninducing) and galactose-containing plates (inducing). They were incubated at 30°C for 2 (glucose) and 4 d (galactose). ProtA, protein A.

Nup159-GFP (not depicted), which are cytoplasmically oriented Nups, were found in a few clustered foci that largely colocalized with the NE. However, the induction of *GAL::NUP170C* significantly increased the mislocalization of these Nups (Figs. 4 and 5). Additionally, Nup188-GFP, which is part of the NPC structural core, showed a significantly altered subcellular distribution upon *GAL::NUP170C* induction in *nup170Δ* cells. In particular, Nup188-GFP was often seen in cytoplasmic foci that were far away from the nuclear compartment, and several of these cytoplasmic foci aligned on NE extensions protruding into the cytoplasm, like pearls on a string (Fig. 4). When Nup170C was overexpressed, the transmembrane Nups Pom34-GFP (Fig. 4) and Pom152-GFP (not depicted) also became mislocalized into the cytoplasm, but rather in a single spot than several foci as observed for Nup188-GFP. Double fluorescence microscopy revealed that the cytoplasmic foci containing CFP-marked Nup188 or Nup159 tend to colocalize with the ER membrane marker Sec61-YFP (Fig. 5). Thus, the cytoplasmic Nup foci induced by Nup170C overproduction are either associated with or close to the membranes containing the ER marker Sec61.

However, the location of Nups that are part of NPC structures facing the nucleoplasm (e.g., Nup2 and Nup1) was not

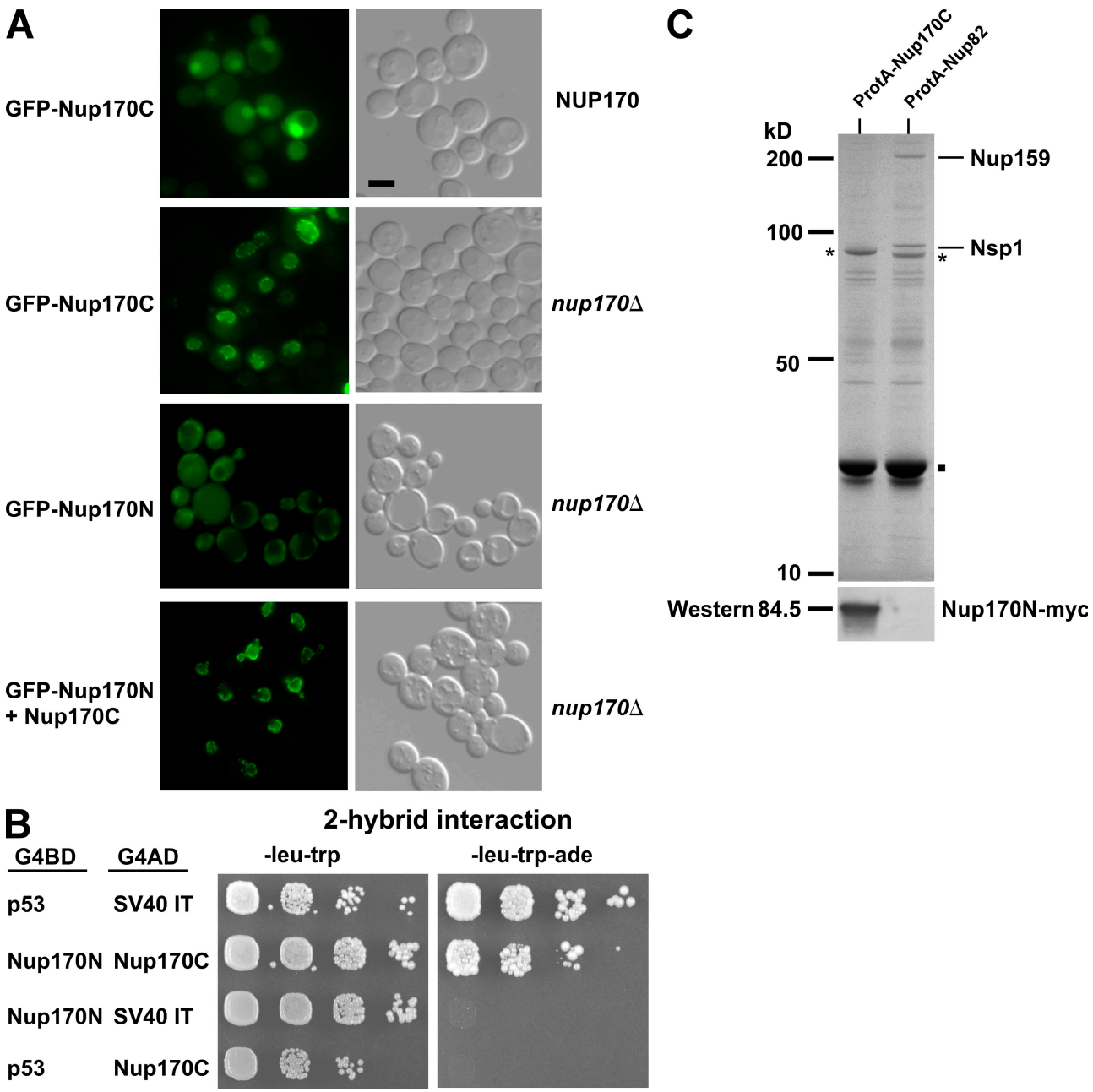

Figure 3. **Nup170C and Nup170N physically and functionally interact with each other.** (A) Nup170C tethers Nup170N to the NE. The indicated GFP-tagged Nup170 domains were expressed under the control of the *NOP1* promoter in the specified strains and analyzed by fluorescence microscopy. Cells are also shown by Nomarski optics. (B) Nup170C and Nup170N show a two-hybrid interaction. The indicated constructs, fused to either the *GAL4* DNA–binding domain (G4BD) or the *GAL4* activation domain (G4AD), were expressed into a reporter yeast strain. Cells were spotted in 10-fold serial dilution steps onto SDC-Trp-Leu (for plating efficiency) or SDC-Trp-Leu-Ade (for two-hybrid interaction) plates and incubated at 30°C for 3 d and 4 d, respectively. (C) Affinity-purified Nup170C coenriched Nup170N. Protein A (ProtA)–tagged Nup170C and protein A–tagged Nup82 were affinity purified from a yeast strain coexpressing myc-tagged Nup170N. The TEV-eluates were analyzed by SDS-PAGE and Coomassie staining (top) and Western blotting (bottom) using anti-myc antibodies to detect Nup170N. Coenriched Nsp1 and Nup159 are indicated on the right. The asterisks label the purified bait proteins, and the dot marks the TEV protease. Bar, 5 μm.

affected by the Nup170C overproduction (Fig. 4 and not depicted). Thus, overproduction of Nup170C affects NPC tethering of Nup1 and Nup2 differently than a *nup170Δ* deletion, which was reported to cause a partial mislocalization of these nucleoplasmic Nups from NPCs (Kenna et al., 1996).

Next, we examined the cells expressing the toxic Nup170C by transmission EM. This analysis revealed electron-dense structures in the cytoplasm that resembled NPCs present in the NE (Fig. S2). However, the diameter of these electron-dense cytoplasmic structures (87 ± 9 nm) was slightly smaller than the size of normal NPCs embedded in the NE (97 ± 11 nm). Thus, it remains open whether the Nup-containing cytoplasmic foci induced by Nup170C overexpression and seen in the fluorescence microscope correspond to these electron-dense structures seen in EM.

In conclusion, the EM structure of Nup170 revealed that it is composed of two distinct structural entities, which is consistent

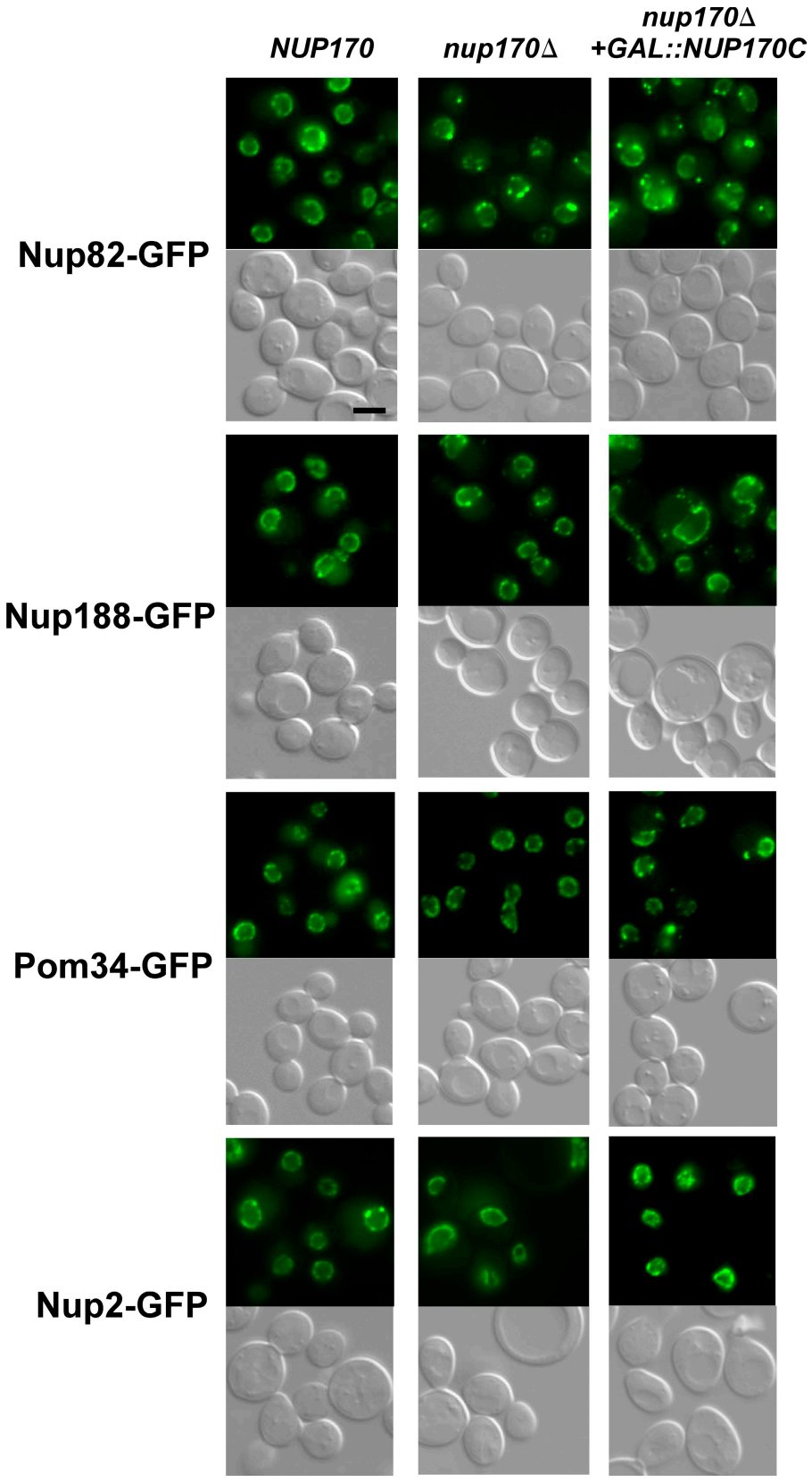

Figure 4. **Overproduction of Nup170C induces a cytoplasmic mislocalization of Nups.** Nup82, Nup188, Pom34, and Nup2, all labeled with GFP at the C terminus by chromosomal integration, were expressed in the wild-type, *nup170Δ*, and *GAL::NUP170C*-overproducing *nup170Δ* strains. Cells were grown in a raffinose-containing (SRC-Leu) medium to an OD_{600} of 0.7 before shift to a galactose-containing (synthetic galactose complete–Leu) medium for 10 h. Cells were inspected in the fluorescence microscope and viewed by Nomarski optics. Counting revealed that 28% of the cells showed mislocalized Nup188-GFP in cytoplasmic foci upon Nup170C overexpression, but only 5% exhibited this phenotype when *GAL::NUP170C* was not induced. 17% of the cells showed Pom34-GFP mislocalized in a cytoplasmic spot upon *GAL::NUP170C* induction versus 2% when *GAL::NUP170C* was not induced. Bar, 2.5 μm.

with the predicted domain separation into an N-terminal β-propeller and a C-terminal α-solenoid. These domains fulfill different functions: the C-terminal part anchors Nup170 to the nuclear pore, and the N terminus is responsible for recruiting and/or retaining certain Nups at the NPCs. Moreover, the overexpression of the Nup170 C-terminal domain generated a toxic phenotype in *nup170Δ* but not *NUP170* cells, which caused a subset of Nups to mislocalize into cytoplasmic foci. In addition,

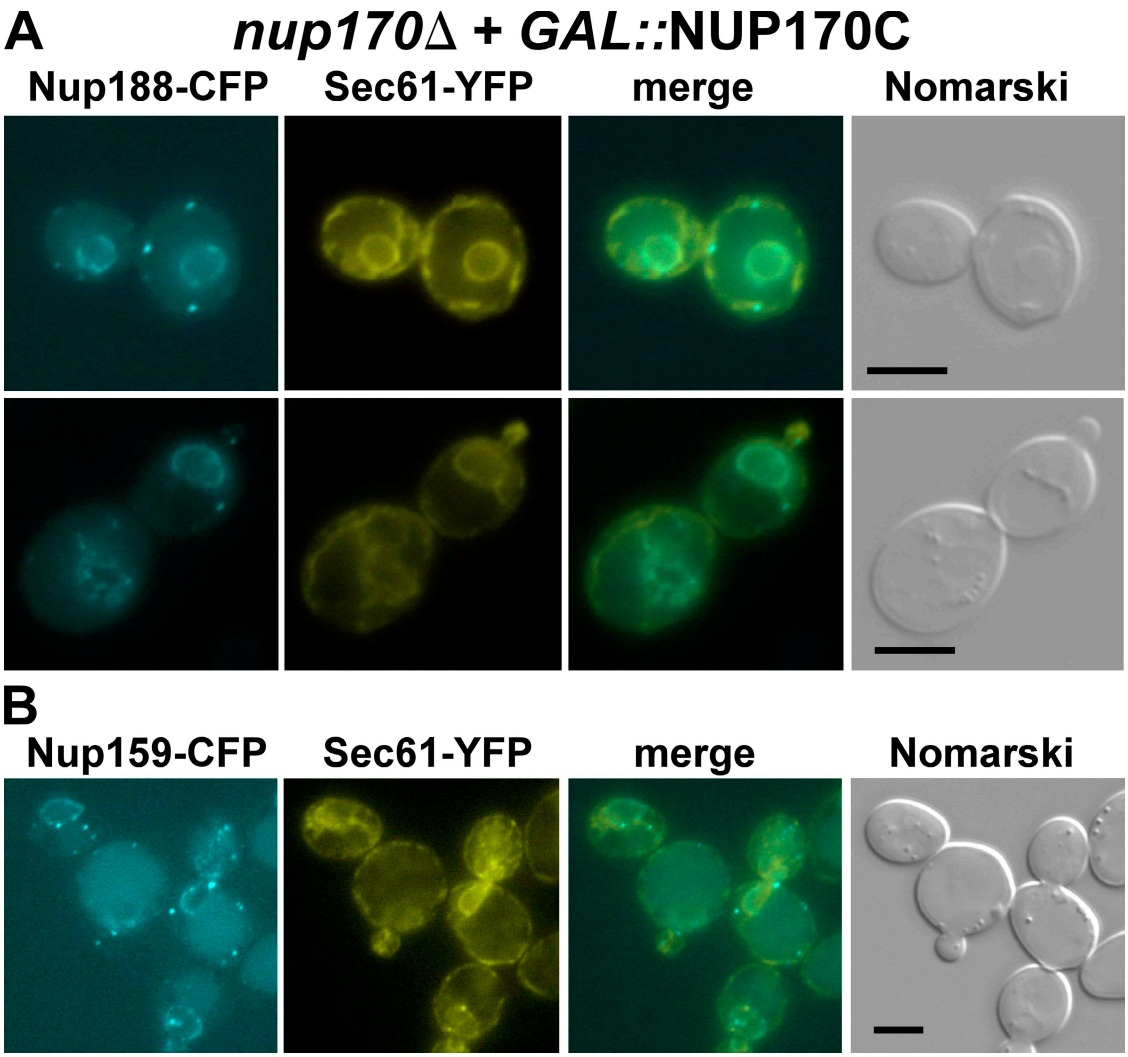

Figure 5. **Cytoplasmic spots containing Nup188 and Nup159 colocalize with the ER marker Sec61 in *GAL::NUP170C*-overproducing cells.** (A and B) Cells expressing Nup188-CFP (A) and Nup159-CFP (B) in a *nup170Δ* strain overproducing *GAL::NUP170C* were analyzed by fluorescence microscopy. Moreover, these strains coexpressed the ER marker Sec61-YFP. Fluorescence microscopic, merged, and Nomarski pictures of representative cells are shown. Bars, 5 µm.

Nup170C overexpression induced nuclear accumulation of poly(A)$^+$ RNA in a significant number of cells, which was not seen in *nup170Δ* cells (Fig. S3). Until now, such an effect of a toxic mutant Nup, which is not seen by its full-length nonessential counterpart, has not been observed. Among the mislocalized Nups were Nups predicted to form the NPC scaffold (Nup188), transmembrane Nups (Pom152 and Pom34), and Nups from the cytoplasmic periphery (Nup159 and Nup82). However, no segregation into cytoplasmic foci was observed for Nups located at the nuclear side of the NPC (Nup1 and Nup2). This finding could implicate that the N terminus of Nup170 (or Nup157) may tether cytoplasmically oriented Nups to the C terminus of Nup170 molecules within the context of the higher order NPC structure.

Under conditions of Nup170C overexpression, the cytoplasmic foci containing GFP-labeled Nups (e.g., Nup188-GFP) sometimes aligned like pearls on a string protruding from the NE. It is possible that the Nup170C domain in concert with other Nups (e.g., Pom34, Pom152, and Nup188) triggers distinct steps in NPC biogenesis that could occur outside of the NE, perhaps at the ER. This possibility is consistent with identified interactions between Pom152 and Nup170 (Alber et al., 2007) and Nup188 and Pom152 (Aitchison et al., 1995). Assuming that these Nup assembly intermediates are first formed outside of the NE, the Nup170N domain may help to target these intermediates to the sites within the nuclear membrane, where the new NPCs form. An evolutionary conserved subcomplex containing Nup170/Nup155 and especially the Nup170-Nup53 assembly has been shown to be crucial for NPC and NE assembly (Hawryluk-Gara et al., 2008). We have found a two-hybrid interaction between the N-terminal domain of Nup170 and Nup53 (unpublished data). Thus, it is possible that upon Nup170C overexpression in yeast, the subcomplex containing Nup170 and Nup53 may not be correctly assembled, and, as a consequence, NPC biogenesis is inhibited. Future studies will be necessary to reveal the composition and exact subcellular location of the observed putative NPC intermediates in the cytoplasm and unravel the precise role of the Nup170 N and C domains in orchestrating both temporally and spatially the complicated steps of NPC biogenesis.

Materials and methods

Yeast strains and yeast genetic methods

The plasmids used in this study are shown in Table S1. The yeast *S. cerevisiae* strains used in this study are listed in Table S2. For the yeast two-hybrid interaction analysis, the plasmid expressing the N domain of Nup170, fused to the *GAL4* DNA–binding domain, and the C-domain of Nup170, fused to the *GAL4* activation domain, were cotransformed into the reporter strain PJ69-4A (James et al., 1996). The interaction was documented by spotting representative transformants in 10-fold serial dilution steps on synthetic dextrose complete (SDC)–Trp-Leu (plating efficiency) and SDC-Trp-Leu-Ade (two-hybrid interaction) plates. C-terminal tagging at the genomic locus was performed as described previously (Longtine et al., 1998; Puig et al., 2001; Janke et al., 2004). Preparation of media, yeast transformation, and genetic manipulations were performed according to established procedures. Analysis of poly(A)$^+$ RNA export was performed at 30°C by in situ hybridization using Cy3-labeled oligo (dT) probes as previously described (Doye et al., 1994).

Affinity purification

Protein purification was performed in a buffer containing 20 mM Tris-HCl, pH 7.5, 150 mM NaCl, 50 mM KOAc, 2 mM $Mg(OAc)_2$, and 0.15% NP-40. The full-length Nup170 chromosomally tagged with a protein A–TEV-Flag construct was purified via affinity purification and size exclusion chromatography. GST-tagged Nup170C (aa 755–1,502) was expressed in *E. coli* and purified to homogeneity by GST affinity purification, TEV cleavage, and ion exchange chromatography. For the TEV cleavage, during the affinity purification of the protein A–tagged C-domain of Nup170, DTT was added to a final concentration of 1 mM to the aforementioned buffer. The samples were separated on NuPAGE SDS 4–12% gradient polyacrylamide gels (Invitrogen) and stained with colloidal Coomassie (Sigma-Aldrich). For EM, an additional anion exchange chromatography of the C domain of Nup170 was performed.

Fluorescence microscopy

Cells were grown to early log phase at 30°C in synthetic raffinose complete (SRC)–Leu and then shifted to 2% galactose for 10 h. Then they were examined by fluorescence microscopy using a microscope (Imager Z1; Carl Zeiss, Inc.) equipped with a 100×/63× NA 1.4 Plan-Apochromat oil immersion lens. Pictures were acquired with a camera (AxioCam MRm; Carl Zeiss, Inc.) and AxioVision 4.3 software (Carl Zeiss, Inc.).

EM, image processing, and fold assignment

Thin-section EM was performed as previously described (Doye et al., 1994). Cells were grown to early log phase at 30°C in SRC-Leu and then shifted to 2% galactose for 10 h. Negative staining for single-particle EM was performed as described previously (Lutzmann et al., 2005). Micrographs were recorded with a field emission gun microscope (CM-200; Phillips) under low dose conditions on a 2K × 2K charge-coupled device camera (TVIPS F224; Tietz) at 200 kV with a nominal magnification of 38,000× (calibrated pixel size, 3.76 Å/pixel) and 50,000×, respectively (calibrated pixel size, 2.86 Å/pixel). For image processing, a total of 4,000 (for Nup170) and 1,500 (for Nup170C) particle images were selected and boxed using the Medical Research Council image-processing package (Crowther et al., 1996) or the SPIDER software package (Frank et al., 1996). All subsequent image processing was performed in Imagic V (Image Science Software GmbH; van Heel et al., 1996). Alignment, iterative refinement of class averages, and the calculation of the 3D maps followed previously described procedures (Lutzmann et al., 2005).

Fold assignment of Nup170 was performed as previously described (Devos et al., 2006). Secondary structure prediction of Nup170 was performed using *psipred* (McGuffin and Jones, 2003), and the 3D model was built by modeller-8 (Sali and Blundell, 1993) from the *hhsearch* (Söding et al., 2005) alignment.

Online supplemental material

Fig. S1 shows the protein expression levels of *NUP170* constructs in the indicated yeast strains. Fig. S2 shows thin-section EM of Nup170C-overexpressing cells. Fig. S3 illustrates that overexpression of Nup170C in *nup170Δ* cells induces an mRNA export defect. Tables S1 and S2 list all of the plasmids and strains, respectively, used in this study. Video S1 displays the 3D EM structure of Nup170. Online supplemental material is available at http://www.jcb.org/cgi/content/full/jcb.200810016/DC1.

We thank the European Molecular Biology Laboratory (EMBL) Heidelberg and Dr. H. Bading (Department of Neurobiology, University of Heidelberg, Heidelberg, Germany) for providing the facilities for transmission EM. We also thank Dr. D. Kressler for providing the plasmid pFA6a-FTpA-HIS3MX4 to generate the double-tagged Nup170 strain and Dr. D. Devos (EMBL Heidelberg) for structure modeling.

E. Hurt is a recipient of grants from the Deutsche Forschungsgemeinschaft (SFB 638/B2) and Fonds der Chemischen Industrie.

Submitted: 6 October 2008
Accepted: 2 April 2009

References

Aitchison, J.D., M.P. Rout, M. Marelli, G. Blobel, and R.W. Wozniak. 1995. Two novel related yeast nucleoporins Nup170p and Nup157p: complementation with the vertebrate homologue Nup155p and functional interactions with the yeast nuclear pore-membrane protein Pom152p. *J. Cell Biol.* 131:1133–1148.

Alber, F., S. Dokudovskaya, L.M. Veenhoff, W. Zhang, J. Kipper, D. Devos, A. Suprapto, O. Karni-Schmidt, R. Williams, B.T. Chait, et al. 2007. The molecular architecture of the nuclear pore complex. *Nature*. 450:695–701.

Beck, M., V. Lucic, F. Forster, W. Baumeister, and O. Medalia. 2007. Snapshots of nuclear pore complexes in action captured by cryo-electron tomography. *Nature*. 449:611–615.

Berke, I.C., T. Boehmer, G. Blobel, and T.U. Schwartz. 2004. Structural and functional analysis of Nup133 domains reveals modular building blocks of the nuclear pore complex. *J. Cell Biol.* 167:591–597.

Crowther, R.A., R. Henderson, and J.M. Smith. 1996. MRC image processing programs. *J. Struct. Biol.* 116:9–16.

Devos, D., S. Dokudovskaya, R. Williams, F. Alber, N. Eswar, B.T. Chait, M.P. Rout, and A. Sali. 2006. Simple fold composition and modular architecture of the nuclear pore complex. *Proc. Natl. Acad. Sci. USA*. 103:2172–2177.

Doye, V., R. Wepf, and E.C. Hurt. 1994. A novel nuclear pore protein Nup133p with distinct roles in poly(A)+ RNA transport and nuclear pore distribution. *EMBO J.* 13:6062–6075.

Fahrenkrog, B., and U. Aebi. 2003. The nuclear pore complex: nucleocytoplasmic transport and beyond. *Nat. Rev. Mol. Cell Biol.* 4:757–766.

Frank, J., M. Radermacher, P. Penczek, J. Zhu, Y. Li, M. Ladjadj, and A. Leith. 1996. SPIDER and WEB: processing and visualization of images in 3D electron microscopy and related fields. *J. Struct. Biol.* 116:190–199.

Galy, V., I.W. Mattaj, and P. Askjaer. 2003. *Caenorhabditis elegans* nucleoporins Nup93 and Nup205 determine the limit of nuclear pore complex size exclusion in vivo. *Mol. Biol. Cell*. 14:5104–5115.

Hawryluk-Gara, L.A., M. Platani, R. Santarella, R.W. Wozniak, and I.W. Mattaj. 2008. Nup53 is required for nuclear envelope and nuclear pore complex assembly. *Mol. Biol. Cell*. 19:1753–1762.

Hodel, A.E., M.R. Hodel, E.R. Griffis, K.A. Hennig, G.A. Ratner, S. Xu, and M.A. Powers. 2002. The three-dimensional structure of the autoproteolytic, nuclear pore-targeting domain of the human nucleoporin nup98. *Mol. Cell*. 10:347–358.

James, P., J. Halladay, and E.A. Craig. 1996. Genomic libraries and a host strain designed for highly efficient two-hybrid selection in yeast. *Genetics*. 144:1425–1436.

Janke, C., M.M. Magiera, N. Rathfelder, C. Taxis, S. Reber, H. Maekawa, A. Moreno-Borchart, G. Doenges, E. Schwob, E. Schiebel, and M. Knop. 2004. A versatile toolbox for PCR-based tagging of yeast genes: new fluorescent proteins, more markers and promoter substitution cassettes. *Yeast*. 21:947–962.

Jeudy, S., and T.U. Schwartz. 2007. Crystal structure of nucleoporin nic96 reveals a novel, intricate helical domain architecture. *J. Biol. Chem.* 282:34904–34912.

Kenna, M.A., J.G. Petranka, J.L. Reilly, and L.I. Davis. 1996. Yeast N1e3p/Nup170p is required for normal stoichiometry of FG nucleoporins within the nuclear pore complex. *Mol. Cell. Biol.* 16:2025–2036.

Kerscher, O., P. Hieter, M. Winey, and M.A. Basrai. 2001. Novel role for a *Saccharomyces cerevisiae* nucleoporin, Nup170p, in chromosome segregation. *Genetics*. 157:1543–1553.

Longtine, M.S., A. McKenzie III, D.J. Demarini, N.G. Shah, A. Wach, A. Brachat, P. Philippsen, and J.R. Pringle. 1998. Additional modules for versatile and economical PCR-based gene deletion and modification in *Saccharomyces cerevisiae*. *Yeast*. 14:953–961.

Lutzmann, M., R. Kunze, K. Stangl, P. Stelter, K.F. Toth, B. Bottcher, and E. Hurt. 2005. Reconstitution of Nup157 and Nup145N into the Nup84 complex. *J. Biol. Chem.* 280:18442–18451.

Mansfeld, J., S. Guttinger, L.A. Hawryluk-Gara, N. Pante, M. Mall, V. Galy, U. Haselmann, P. Muhlhausser, R.W. Wozniak, I.W. Mattaj, et al. 2006. The conserved transmembrane nucleoporin NDC1 is required for nuclear pore complex assembly in vertebrate cells. *Mol. Cell*. 22:93–103.

Marelli, M., J.D. Aitchison, and R.W. Wozniak. 1998. Specific binding of the karyopherin Kap121p to a subunit of the nuclear pore complex containing Nup53p, Nup59p, and Nup170p. *J. Cell Biol.* 143:1813–1830.

Marelli, M., C.P. Lusk, H. Chan, J.D. Aitchison, and R.W. Wozniak. 2001. A link between the synthesis of nucleoporins and the biogenesis of the nuclear envelope. *J. Cell Biol.* 153:709–724.

McGuffin, L.J., and D.T. Jones. 2003. Benchmarking secondary structure prediction for fold recognition. *Proteins*. 52:166–175.

Melcak, I., A. Hoelz, and G. Blobel. 2007. Structure of Nup58/45 suggests flexible nuclear pore diameter by intermolecular sliding. *Science*. 315:1729–1732.

Puig, O., F. Caspary, G. Rigaut, B. Rutz, E. Bouveret, E. Bragado-Nilsson, M. Wilm, and B. Seraphin. 2001. The tandem affinity purification (TAP) method: a general procedure of protein complex purification. *Methods*. 24:218–229.

Rout, M.P., J.D. Aitchison, A. Suprapto, K. Hjertaas, Y. Zhao, and B.T. Chait. 2000. The yeast nuclear pore complex: composition, architecture, and transport mechanism. *J. Cell Biol.* 148:635–651.

Sali, A., and T.L. Blundell. 1993. Comparative protein modelling by satisfaction of spatial restraints. *J. Mol. Biol.* 234:779–815.

Schrader, N., P. Stelter, D. Flemming, R. Kunze, E. Hurt, and I.R. Vetter. 2008. Structural basis of the nic96 subcomplex organization in the nuclear pore channel. *Mol. Cell*. 29:46–55.

Shulga, N., N. Mosammaparast, R. Wozniak, and D.S. Goldfarb. 2000. Yeast nucleoporins involved in passive nuclear envelope permeability. *J. Cell Biol.* 149:1027–1038.

Söding, J., A. Biegert, and A.N. Lupas. 2005. The HHpred interactive server for protein homology detection and structure prediction. *Nucleic Acids Res.* 33:W244–248.

Stoffler, D., B. Fahrenkrog, and U. Aebi. 1999. The nuclear pore complex: from molecular architecture to functional dynamics. *Curr. Opin. Cell Biol.* 11:391–401.

Tran, E.J., and S.R. Wente. 2006. Dynamic nuclear pore complexes: life on the edge. *Cell*. 125:1041–1053.

van Heel, M., G. Harauz, E.V. Orlova, R. Schmidt, and M. Schatz. 1996. A new generation of the IMAGIC image processing system. *J. Struct. Biol.* 116:17–24.

Weirich, C.S., J.P. Erzberger, J.M. Berger, and K. Weis. 2004. The N-terminal domain of Nup159 forms a beta-propeller that functions in mRNA export by tethering the helicase Dbp5 to the nuclear pore. *Mol. Cell*. 16:749–760.